Chapter 4
Macroscopic Models

Macroscopic traffic flow models forms arguably the largest family in the model tree, see page 15. They describe traffic flow as if it were a continuum flow and are often compared to, or derived in analogy with, continuum models for fluids. Individual vehicles are not modeled, however aggregated variables such as (average) density and (average) flow are used.

After reading this chapter, the reader will understand the basics of the most popular macroscopic models, including their main features. They understand why and how extensions of macroscopic models such as higher order models, multi-class models and extensions using bounded acceleration or capacity drop, will improve them. The reader will also be able to adapt a simple model in these directions. They can reflect on desired properties of such models, including anisotropy. Finally, the reader will become familiar with the Eulerian and Lagrangian coordinate systems and will be able to reflect on their (dis)advantages.

4.1 Kinematic Wave Models

Macroscopic traffic flow models were first introduced by Lighthill and Whitham (1955b) and, independently (Richards 1956). Their model is the prototype kinematic wave model and was named the LWR model later. The dynamics of traffic is described by a partial differential equation, which models the conservation of vehicles:

$$\frac{\partial \rho}{\partial t} + \frac{\partial q}{\partial x} = 0 \tag{4.1}$$

and a fundamental relation $q = Q(\rho)$. The system of equations is closed with the relation between flow q, density ρ and speed v: $q = \rho v$. This model is closely related to other models for fluid flow, which often look very similar, with just an

© Springer International Publishing AG, part of Springer Nature 2019

F. Kessels, *Traffic Flow Modelling*, EURO Advanced Tutorials
on Operational Research, https://doi.org/10.1007/978-3-319-78695-7_4

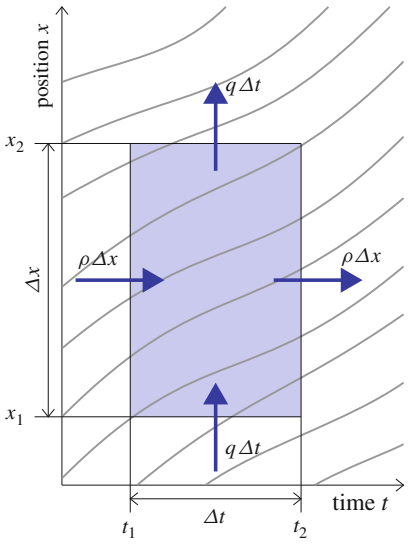

Fig. 4.1 Graphical derivation of the conservation equation in the kinematic wave model using vehicle trajectories and a control volume

other type of density-flow relation. The LWR model, was even introduced as Part 2 (Lighthill and Whitham 1955b) of a pair of articles, the first one titled 'On kinematic waves I: Flood movement in long rivers' (Lighthill and Whitham 1955a).

4.1.1 Graphical Derivation

The vehicle conservation equation (4.1) can be derived using vehicle trajectories in a control volume as illustrated in Fig. 4.1. The number of vehicles entering the control volume (inflow) equals the number of vehicles leaving it (outflow). This can be written as:

$$\underbrace{\int_{x_1}^{x_2} \rho(t_1, x)\,\mathrm{d}x}_{\text{inflow from left}} + \underbrace{\int_{t_1}^{t_2} q(t, x_1)\,\mathrm{d}t}_{\text{inflow from below}} = \underbrace{\int_{x_1}^{x_2} \rho(t_2, x)\,\mathrm{d}x}_{\text{outflow to right}} + \underbrace{\int_{t_1}^{t_2} q(t, x_2)\,\mathrm{d}t}_{\text{outflow to above}} \tag{4.2}$$

We decrease the control volume to an infinitesimal volume: $x_2 = x_1 + \Delta x \to x_1$ and $t_2 = t_1 + \Delta t \to t_1$. Because the volume is small, we may assume density ρ and flow q are constant.[1] Consequently, $\int_{x_1}^{x_2} \rho(t, x)\mathrm{d}x \to \rho(t, x_1)\Delta x$ and $\int_{t_1}^{t_2} q(t, x)\mathrm{d}t \to q(t_1, x)\Delta t$. Furthermore, rewriting (4.2) yields:

$$\frac{\rho(t_1 + \Delta t, x) - \rho(t_1, x)}{\Delta t} + \frac{q(t, x_1 + \Delta x) - q(t, x_1)}{\Delta x} = 0 \tag{4.3}$$

[1] This assumption is related to the continuum assumption, stating that the flow can be described as if it were a continuum instead of individual particles. The validity of this assumption is discussed in more detail in Sect. 7.1.1.

We now recall the definition of the partial derivatives of $f = f(y, z)$:

$$\frac{\partial}{\partial y} f(y,z) = \lim_{\Delta y \to 0} \frac{f(y+\Delta y, z) - f(y,z)}{\Delta y},$$
$$\frac{\partial}{\partial z} f(y,z) = \lim_{\Delta z \to 0} \frac{f(y, z+\Delta z) - f(y,z)}{\Delta z} \tag{4.4}$$

We apply this definition (4.4) to the infinitesimal control volume and find the conservation equation (4.1).

4.1.2 Method of Characteristics

To solve the equations of the kinematic wave model, different methods can be applied. We introduce the method of characteristics because it gives a good insight into the behaviour of the model and into how the model can be extended for more realistic results. Furthermore, Chap. 5 will discuss numerical methods that can be applied in computer simulations.

4.1.2.1 Characteristics

An important property of any traffic flow model is the speed and direction of information: if there is a discontinuity or a disturbance, at which speed does it travel to influence other vehicles, and in which direction? Sometimes, it travels with the vehicles, in other cases information will travel upstream, against the travel direction of the vehicles.

In the kinematic wave model, it is relatively easy to analyse the characteristic velocity. In this context, characteristics are lines of constant density. In general, in partial differential equations, characteristics, or characteristic waves, or characteristic curves, are curves in the (t, x) plane along which the equation simplifies in a certain way. This touches upon an important difference between the kinematic wave model and other non-linear hyperbolic partial differential equations, on one hand, and linear constant-coefficient hyperbolic partial differential equations such as the advection equation on the other hand:

$$\frac{\partial \rho}{\partial t} + v \frac{\partial \rho}{\partial x} = 0 \tag{4.5}$$

In the advection equation (4.5), the characteristic velocity equals the flow velocity v and characteristic curves are straight lines at which density is constant. However, in the kinematic wave model (4.1), characteristic velocity depends on the actual traffic state. To see this, we rewrite the conservation equation (4.1) in quasilinear form:

$$\frac{\partial \rho}{\partial t} + \frac{\partial q}{\partial x} = \frac{\partial \rho}{\partial t} + \frac{\mathrm{d}Q}{\mathrm{d}\rho} \frac{\partial \rho}{\partial x} = 0 \tag{4.6}$$

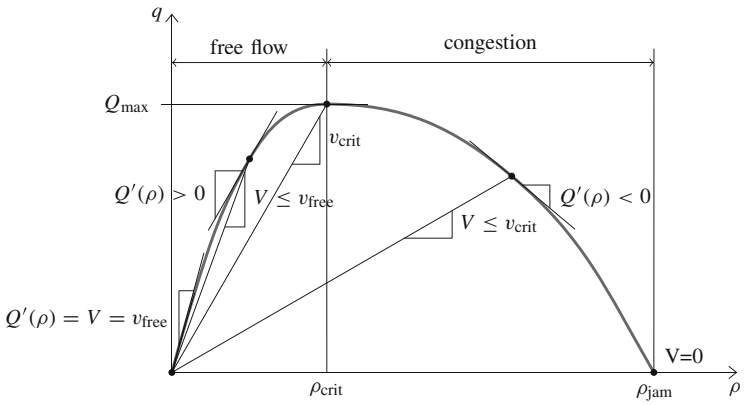

Fig. 4.2 Fundamental diagram with indication of characteristic velocities: in free flow, characteristic velocities are positive, in the congestion branch, they are negative

Again, at the characteristic curves, density is constant. However, the characteristic velocity does not always equal the flow velocity, instead it is:

$$\frac{\mathrm{d}Q}{\mathrm{d}\rho} = Q'(\rho) = V(\rho) + \rho V'(\rho) \tag{4.7}$$

We note that the characteristic velocity thus equates to the slope of the $Q(\rho)$ fundamental diagram. Assuming a traditionally shaped continuous and concave fundamental diagram (see Fig. 4.2) with an increasing free flow branch and a decreasing congestion branch the following holds:

- At zero density ($\rho = 0$), vehicle velocity equals characteristic velocity: $\left.\frac{\mathrm{d}Q}{\mathrm{d}\rho}\right|_{\rho=0} = V(0) = v_{max}$.
- If traffic is in free flow ($\rho \leq \rho_{crit}$), then the slope of the characteristic curve is positive and information moves in the same direction as the vehicles.
- If traffic is in congestion ($\rho > \rho_{crit}$), then the slope of the characteristic curve is negative and information moves in the direction opposite of the direction of the vehicles.

4.1.2.2 Shock Waves

Characteristics, as described in the previous paragraph, can move in either direction: upstream or downstream—backward or forward and at various speeds. Therefore, if the above is applied in a naive way to an initial value problem with increasing densities, characteristics may also intersect, see e.g. Fig. 4.3. An other way of looking at this is shown in Fig. 4.4. The initial densities propagate at different

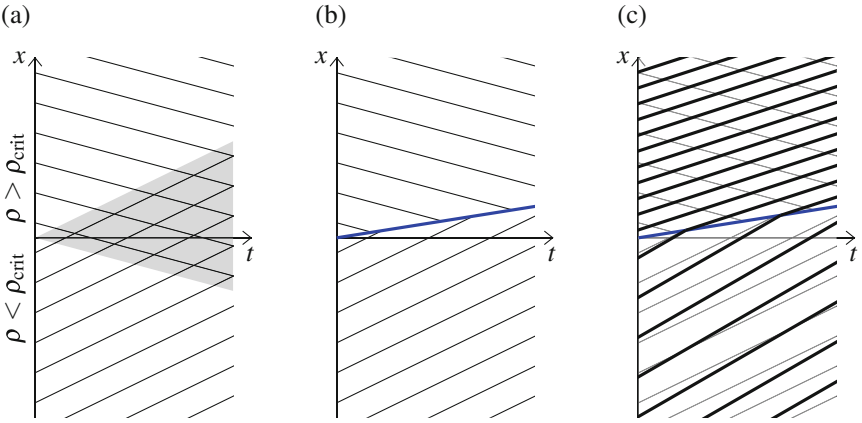

Fig. 4.3 Example of intersecting characteristics and the creation of a shock wave. (**a**) Intersecting characteristics (gray area). (**b**) Characteristics and shock wave (thick blue line). (**c**) Characteristics, shock wave and vehicle trajectories (thick lines)

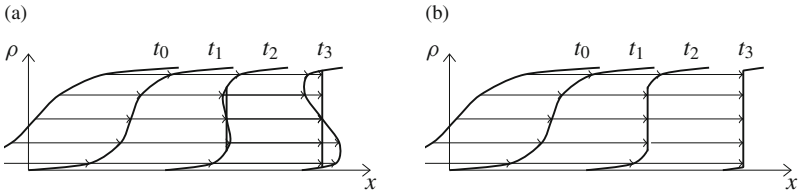

Fig. 4.4 Example of focussing of a deceleration wave, resulting in (unrealistic) triple valued solutions and a (realistic) shock. (**a**) Triple valued solution at $t = t_2$ and $t = t_3$. (**b**) Shock

speeds, leading to triple valued solutions. This is where shock wave theory comes into play. Shock waves—also known as kinematic waves—are formed at the boundary between characteristics that would otherwise intersect or lead to triple valued solutions.

To calculate the velocity of a shock wave, we first observe that vehicles may—and often do—travel at a velocity unequal to the shock wave velocity v_{shock}. Furthermore, the flux into the shock $\rho_{\text{upstream}}(v_{\text{upstream}} - v_{\text{shock}})$, must equal the flux leaving the shock $\rho_{\text{downstream}}(v_{\text{downstream}} - v_{\text{shock}})$. Therefore, the velocity of the shock wave is:

$$\begin{aligned} v_{\text{shock}} &= \frac{\rho_{\text{upstream}} v_{\text{upstream}} - \rho_{\text{downstream}} v_{\text{downstream}}}{\rho_{\text{upstream}} - \rho_{\text{downstream}}} \\ &= \frac{q_{\text{upstream}} - q_{\text{downstream}}}{\rho_{\text{upstream}} - \rho_{\text{downstream}}} \end{aligned} \tag{4.8}$$

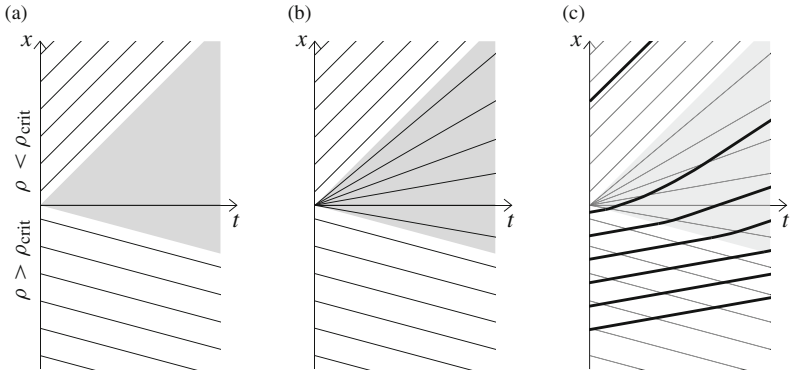

Fig. 4.5 Example of 'missing' characteristics and the creation of a rarefaction wave. (**a**) Characteristics (lines) and area with unknown characteristics (gray). (**b**) Characteristics, also in the rarefaction wave area. (**c**) Characteristics and trajectories (thick lines)

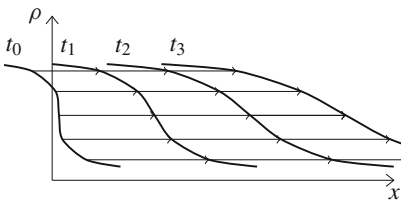

Fig. 4.6 Example of a rarefaction wave

4.1.2.3 Rarefaction Waves

Finally, it can also occur that characteristics move away from each other, yielding no solution at all in certain areas, see e.g. Figs. 4.5 and 4.6. It occurs at a discontinuity with a decreasing density in x-direction. This is where the concept of entropy maximisation comes into play. In these areas, entropy maximisation yields that vehicles drive as fast as possible, given the traffic state. This is also called the 'drive impulse' (Ansorge 1990). The traffic state at (t, x)—any point between the characteristics emanating from either the downstream or the upstream region—can now be determined by solving:

$$\frac{x - x_0}{t - t_0} = Q'(\rho) \tag{4.9}$$

with an initial discontinuity at (t_0, x_0). This equation has a unique solution if and only if the $Q(\rho)$ fundamental relation is strictly concave. If, however, it is concave, but not strictly concave, the entropy condition states that the solution with the highest flux is chosen, i.e. the state that corresponds to the state on the fundamental diagram closest to capacity.

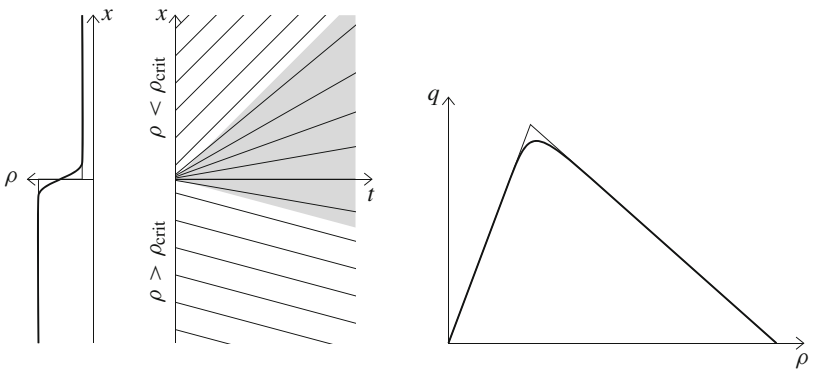

Fig. 4.7 Example a rarefaction wave constructed using a smooth approximation of the initial conditions (on the left) and of the fundamental diagram (on the right)

An other way to approach the issue with the lack of characteristics emanating from the initial conditions, is to use a smooth approximation, see Fig. 4.7. A discontinuity in the initial density at location $x = 0$ is approximated as:

$$\rho(0,x) = \begin{cases} \rho_{\text{upstream}} & \text{if } x \leq -\varepsilon \\ \frac{\rho_{\text{upstream}}+\rho_{\text{upstream}}}{2\varepsilon} x & \text{if } -\varepsilon < x < \varepsilon \\ \rho_{\text{downstream}} & \text{if } x \geq \varepsilon \end{cases} \tag{4.10}$$

With small $\varepsilon > 0$. Note that if $\varepsilon \to 0$, we get back a discontinuity, with on one side $\rho = \rho_{\text{upstream}}$ and on the other side $\rho = \rho_{\text{downstream}}$. Furthermore, any discontinuity in the differentiability of the fundamental relation, is approximated as being continuously differentiable. For example, the bilinear fundamental relation would be approximated as:

$$Q(\rho) = \begin{cases} \rho v_{\text{free}} & \text{if } \rho \leq \rho_{\text{crit}} - \delta \\ \tilde{Q}(\rho) & \text{if } \rho_{\text{crit}} - \delta < \rho < \rho_{\text{crit}} + \delta \\ \frac{\rho_{\text{crit}} v_{\text{free}}}{\rho_{\text{jam}} - \rho_{\text{crit}}} (\rho_{\text{jam}} - \rho) & \text{if } \rho \geq \rho_{\text{crit}} + \delta \end{cases} \tag{4.11}$$

With small $\delta > 0$. $\tilde{Q}(\rho)$ is chosen such that $Q(\rho)$ is continuous and continuously differentiable. If we now apply the method of characteristics, we find characteristics with all slopes between v_{free} and $-\frac{\rho_{\text{crit}} v_{\text{free}}}{\rho_{\text{jam}} - \rho_{\text{crit}}}$ emanating from the (now smoothened) discontinuity at $x = 0$. And the expansion wave becomes apparent.

4.1.2.4 Constructing Solutions

The method of characteristics as described above is applied to the typical test case of a traffic light problem. It is formulated as an initial value on an infinitely long road:

$$\rho(0,x) = \begin{cases} 0 & \text{if } x > 0 \\ \rho_{\text{jam}} & \text{if } -L < x \leq 0 \\ \rho_{\text{upstream}} & \text{if } x \leq -L \end{cases} \tag{4.12}$$

with L the length of the queue of vehicles waiting for the traffic light to turn green at $t = 0$ and $\rho_{\text{upstream}} < \rho_{\text{crit}}$ the density upstream of the queue. See also Fig. 4.8a. To simplify calculations, a bilinear fundamental diagram is applied. The solution—as shown in Fig. 4.8—is constructed with the following steps:

1. Determine characteristic velocities at time $t = 0$.
2. Identify initial locations of shock and expansion waves.
3. Determine the shock wave velocity.
4. Find whether and where the shock wave and the expansion wave meet and the behaviour after this.
5. Fill in all traffic states between the boundaries that were just determined.

Other typical problems that can be solved using the method of characteristics are Riemann initial value problems and certain boundary value problems. The interested reader is encouraged to practice with these cases in the problem set (Problems 4.1 and 4.2).

4.1.3 Simulation Results with the Kinematic Wave Model

The results of a simple simulation are shown in Fig. 4.9. The test case is the same as used for microscopic models in the previous chapter, most notably Sect. 3.2.2. It shows vehicles on a 800 meter long ring road. They are waiting in a queue of length 200 meters until the first one starts driving at $t = 0$. They drive on a ring road and thus the first vehicle essentially follows the last one. A linear-parabolic fundamental diagram is applied, with parameters as in Table 4.1. Furthermore, the table also shows the parameter values of the numerical method, an explicit Lagrangian scheme. The relevance of the numerical method is discussed in Chap. 5.

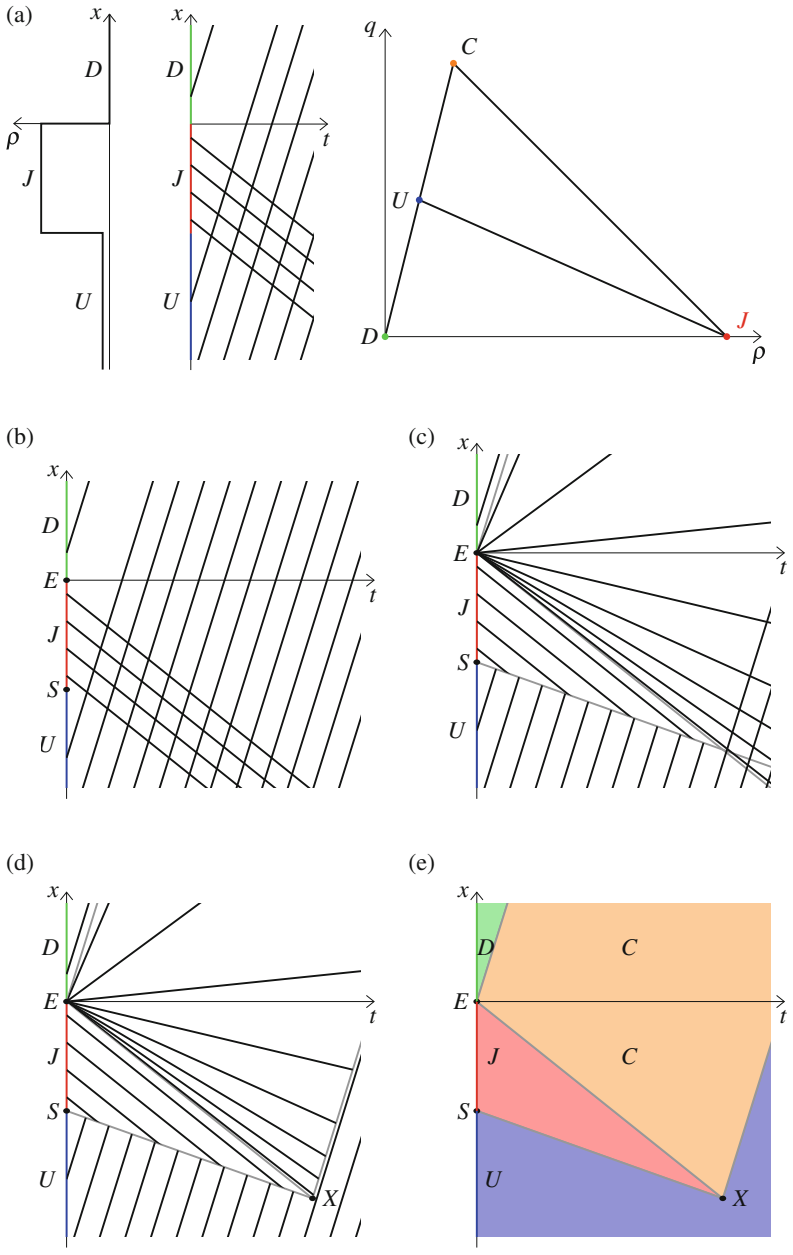

Fig. 4.8 Example of the application of the method of characteristics to a traffic light problem. (**a**) Step 1: initial conditions (left), fundamental diagram (right) and characteristics (center). (**b**) Step 2: locations of shock and expansion wave. (**c**) Step 3: shock wave velocity and expansion wave. (**d**) Step 4: after shock and expansion wave meet (X). (**e**) Step 5: solution in the form of traffic state

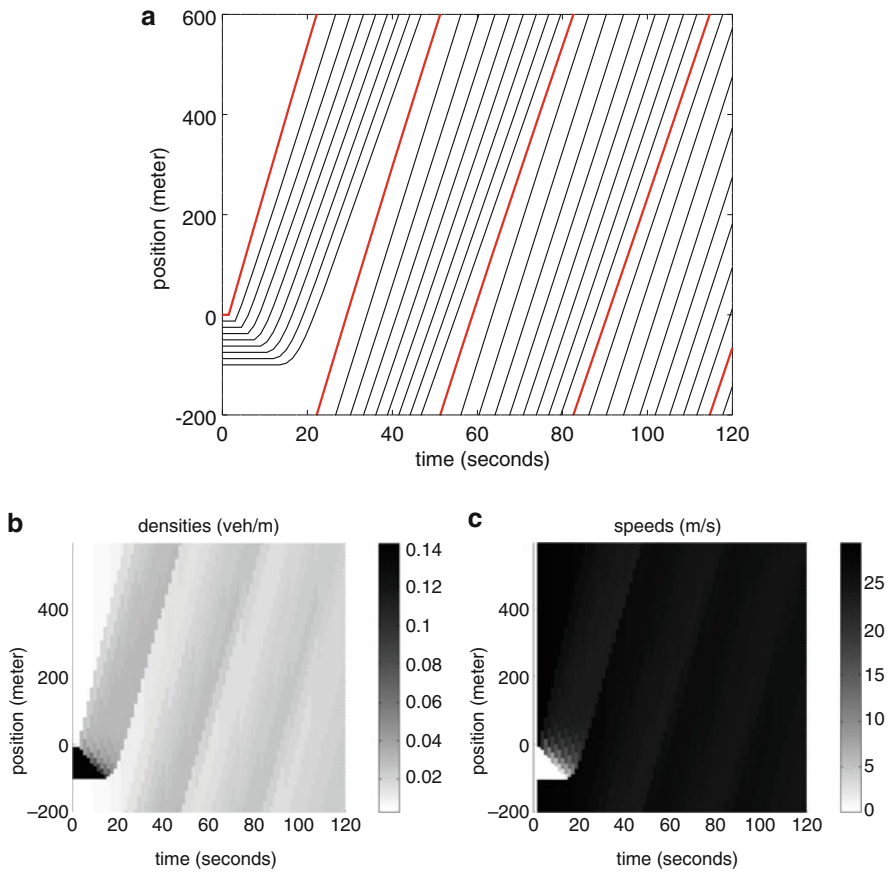

Fig. 4.9 Simulation results with the kinematic wave model with parabolic-linear fundamental diagram. The test case is a ring road, with an initial queue that dissolves, as described in Sect. 4.1.3. The same results are presented in different ways. (**a**) Trajectories of 'vehicle groups': they are not actual vehicle trajectories, but of groups of $\Delta n \approx 1.79$ vehicles. The thick red trajectory is that of the first vehicle group that starts driving at $t = 0$. The other trajectories (black) are of groups that were waiting in a queue behind the first one. (**b**) Densities. (**c**) Speeds

Table 4.1 Parameter values of the linear-parabolic fundamental diagram and numerical scheme applied to the kinematic wave model

Maximum speed $v_{\max}$	30 m/s
Critical speed v_{crit}	$\frac{4}{5}v_{\max} = 24$ m/s
Jam density ρ_{jam}	$\frac{1}{7} \approx 0.14$ veh/m
Critical density ρ_{jam}	$\frac{1}{5}\rho_{\text{jam}} \approx 0.029$ veh/m
Time step size Δt	1.5 s
Vehicle group size Δn	≈ 1.79
CFL number ν	0.9

4.1.4 Critique and Adaptations of the Kinematic Wave Model

Because of its simplicity the LWR model has received both much attention and critique. The model tree shows that this resulted in many offshoots. The main drawback is that vehicles are assumed to attain the new equilibrium velocity immediately after a change in the traffic state, which implies infinite acceleration. This problem is addressed by:

higher order models with an added speed equation, see Sect. 4.3
bounded acceleration and hysteresis as extension to LWR, sometimes modelled as a capacity drop, see Sect. 4.5

An other drawback of the LWR model is that breakdown (the transition from the free flow regime to the congestion regime) always occurs at the same density and leads to the same outflow after breakdown. This is addressed by:

heterogeneity by introducing different types of vehicles or drivers, driving according to different fundamental diagrams, see Sect. 4.2
stochasticity using breakdown probabilities (Hoogendoorn et al. 2009) or via other probability distributions (Jabari and Liu 2012, 2013) (not discussed in detail in this book).
multi-lane kinematic wave models in which vehicle flow is separated into flows on each lane and between the lanes—as opposed to a 'single pipe flow'. The multi-class model (Daganzo et al. 1997) is an example. Other multi-lane models (Laval and Daganzo 2006; Jin 2010) are not discussed in detail in this book.

Finally, the approaches can be combined, for example by multi-class or higher order models with capacity drop. We will not discuss these models in detail because combining multiple extensions is usually rather straightforward and does not add much extra theoretical insights. However, combining approaches can be useful to obtain realistic simulation results for a wider range of applications and scenarios.

4.2 Multi-Class Kinematic Wave Models

In the last one to two decades, the branch of multi-class kinematic wave models has developed quickly. This follows the earlier development of other types of multi-class models (micro- and mesoscopic, higher-order macroscopic).

Multi-class kinematic wave models all consist of a system of conservation equations. There is one conservation equation for each of the U classes:

$$\frac{\partial \rho_u}{\partial t} + \frac{\partial q_u}{\partial x} = 0 \tag{4.13}$$

with ρ_u the class specific density of class u, $q_u = \rho_u v_u$ the class specific flow and v_u the class specific velocity. The class specific velocity is defined differently for

each model, but they can all be cast into the following form:

$$v_u = V_u(\rho_1, \rho_2, \ldots, \rho_U) \tag{4.14}$$

This implies that the class specific velocity only depends on the current class specific densities, and not on any previous state. Therefore, these models are classified as kinematic wave models.

In the simplest—and oldest—multi-class kinematic wave models the speed depends on the total density:

$$v_u = V_u\left(\rho_1, \rho_2, \ldots, \rho_U\right) = V_u\left(\sum_{u=1}^{U} \rho_u\right) \tag{4.15}$$

Furthermore, the fundamental relation is scaled differently for each class, see Fig. 4.10a:

$$v_u = V_u\left(\sum_{u=1}^{U} \rho_u\right) = \frac{v_{u,\max}}{v_{1,\max}} V_1\left(\sum_{u=1}^{U} \rho_u\right) \tag{4.16}$$

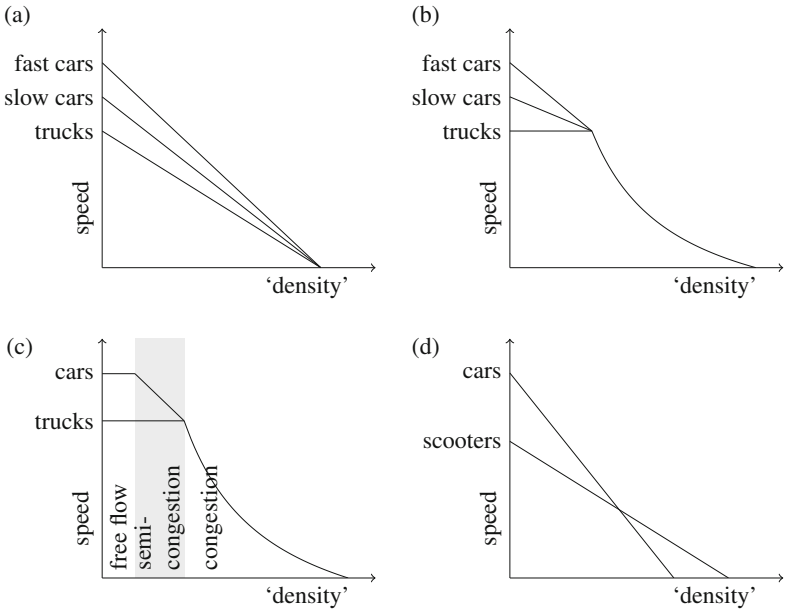

Fig. 4.10 Typical density-speed fundamental diagrams of multi-class macroscopic models. The precise definition of 'density' differs per model: it could be the total density $\sum_u \rho_u$, the weighted sum of the class specific densities, $\sum_u \eta_u \rho_u$, or even some other increasing density function $\rho(\rho_1, ..., \rho_U)$. (**a**) Basic multi-class model with scaled fundamental diagram. (**b**) Fastlane or cross section of multi-dimensional fundamental diagram. (**c**) Three regime model. (**d**) Porous flow model

The model tree shows that Wong and Wong (2002) were the first to introduce such a multi-class kinematic wave model.

4.2.1 Multi-Dimensional Fundamental Diagram

Later models apply a multi-dimensional fundamental diagram, to include the difference in length between the classes. Effectively, these models scale both axes of the fundamental relation differently for each class. In the case of two classes, this leads to a three dimensional fundamental relation (see Figs. 2.13(d), 4.10b). For example, the fundamental diagram introduced by Chanut and Buisson (2003) is a scaled version of the linear-parabolic fundamental diagram (2.3):

$$v_u = V_u(\rho_1, \rho_2) \begin{cases} v_{u,\max} - \frac{v_{u,\max} - v_{\text{crit}}}{\rho_{\text{crit}}(\rho_1,\rho_2)} & \text{if } \rho_1+\rho_2 < \rho_{\text{crit}}(\rho_1, \rho_2) \\ \frac{\rho_{\text{crit}}(\rho_1,\rho_2) v_{\text{crit}}}{\rho_{\text{jam}}(\rho_1,\rho_2)\rho_{\text{crit}}(\rho_1,\rho_2)} \left(\frac{\rho_{\text{jam}}(\rho_1,\rho_2)}{\rho_1+\rho_2} - 1 \right) & \text{if } \rho_1+\rho_2 \geq \rho_{\text{crit}}(\rho_1, \rho_2) \end{cases} \tag{4.17}$$

with state dependent (scaled) critical density and jam density, respectively:

$$\rho_{\text{crit}}(\rho_1, \rho_2) = \beta \rho_{\text{jam}}(\rho_1, \rho_2) \quad \text{and} \quad \rho_{\text{jam}}(\rho_1, \rho_2) = \frac{\rho_1 + \rho_2}{L_1\rho_1 + L_2\rho_2} \tag{4.18}$$

with $\beta < 0.5$ and L_1 and L_2 the gross vehicle lengths of class 1 and 2, respectively. Therefore, when there are no vehicles of class 2 present (i.e. $\rho_2 = 0$), then the jam density parameter is the inverse of the vehicle length of class 1: $\rho_{\text{jam}}(\rho_1, 0) = 1/L_1$. Similarly, when there are no vehicles of class 1, then $\rho_{\text{jam}}(0, \rho_2) = 1/L_2$.

4.2.2 Fastlane

Fastlane is an other offshoot in the branch of multi-class kinematic wave models (van Lint et al. 2008; van Wageningen-Kessels et al. 2014). An 'effective density' is computed and this is used as input for the fundamental relation. The fundamental relation now expresses the class specific velocity as a function of the effective density, see Fig. 4.10b. The effective density is a weighted summation of all class specific densities:

$$\rho = \sum_u \eta_u(\rho)\rho_u \tag{4.19}$$

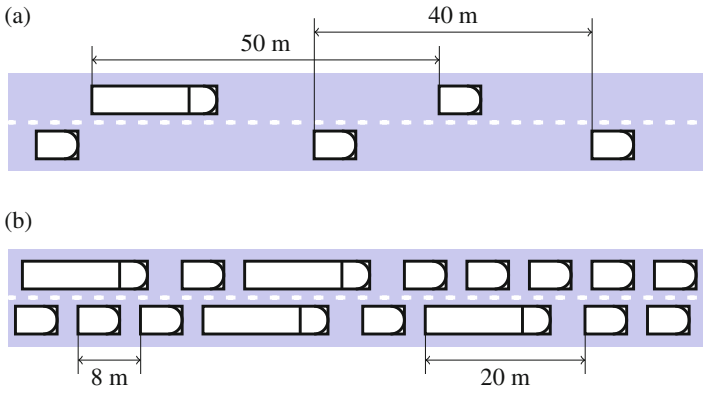

Fig. 4.11 Example illustrations of pce-values. Vehicles drive to the right, cars (short) and trucks (long) are present. In both examples, the truck is longer than the car and the gap (distance *between* two vehicles) is similar for cars and trucks. (**a**) Few vehicles with large spacings: free flow. The space occupancy of a truck (50 m) is a bit higher than that of a car (40 m). This is because the gap is much higher than the vehicle length and thus the vehicle length contributes relatively little to the space occupancy. In this example, the pce value of a truck is $\eta_{\text{truck}} = 50/40 = 1.25$. (**b**) Many vehicles, with small spacings: congestion. The space occupancy of a truck (20 m) is much higher than that of a car (8 m). This is because the truck is longer, but the gap is very similar for both cars and trucks. In this example, the pce value of a truck is be $\eta_{\text{truck}} = 20/8 = 2.5$

with η_u the state-dependent passenger car equivalent (pce) value:

$$\eta_u(\rho) = \frac{L_u + T_u v_u(\rho)}{L_1 + T_1 v_1(\rho)} \tag{4.20}$$

The idea behind the pce value is as follows: Passenger cars have a pce value of 1. Other pce values in Fastlane depend on the actual traffic state. The approach takes into account that adding one truck into the mix, will have a larger effect on the flow than adding one car. Furthermore, and this is unique for Fastlane, a truck takes up more space than a car, but this effect is much larger at high densities and low speeds than it is at low densities and high speeds. This is illustrated in Fig. 4.11.

We note that the presented formulation of Fastlane includes an implicit density function (4.19): to calculate the density, the pce values need to be known, for which the densities are needed (4.20). An alternative formulation of Fastlane that is more practical to apply and more theoretically sound (because it does not have this implicit self-reference)—albeit much more complicated at first sight—is presented by van Wageningen-Kessels et al. (2014).

4.2.3 Models with Three Regimes

A different approach to modelling the behaviour of classes that share a (multi-lane) road is by assuming that the flow is always in a 'lane distribution equilibrium'. In this equilibrium, the vehicles distribute themselves over the lanes in such a way that any other distribution would lead to lower speeds for at least one of the classes. Furthermore, all vehicles drive as fast as possible, on the fraction of the road that is available to them. The most simple of this type of models is the two-class and two-lane model by Daganzo (2002). The terminology of 'slugs' (slow cars) and 'rabbits' (fast cars) is used. Slugs always stay on the outer lane. Rabbits can use both lanes and chose among them based on a user equilibrium. This gives rise to 3 possible 'regimes', see also Fig. 4.10c:

free flow If there are few cars, fast cars will remain on the inner lane and drive at their maximum speed.

semi-congestion If the number of fast cars increases slightly above the density threshold for their maximum speed (critical density), then their speed decreases, but they will stay in the inner lane.

congestion If the number of fast cars increases even more and their speed drops below the maximum speed of the slow cars, there is no advantage anymore in only staying in the inner lane. In fact, the fastest cars will start sharing the outer lane with the slow cars. In this situation, both types of cars will drive at the same speed.

This leads to the following density speed relationships:

$$\begin{array}{ll} v_1 = v_{1,\max}, \quad v_2 = v_{2,\max} & \text{free flow, 2 pipe} \\ v_1 = w_1 \left(\frac{\rho_{\text{jam}}}{\rho_1} - 1 \right), \quad v_2 = v_{2,\max} & \text{semi-congestion, 2 pipe} \\ v_1 = v_2 = \frac{w_1 w_2}{w_1 + w_2} \left(\left(\frac{1}{\rho_1} + \frac{1}{\rho_2} \right) \rho_{\text{jam}} - 1 \right) & \text{congestion, 1 pipe} \end{array} \tag{4.21a}$$

with congestion wave speed:

$$w_u = \frac{\rho_{\text{crit}} v_{u,\max}}{\rho_{\text{jam}} - \rho_{\text{crit}}} \tag{4.22}$$

and ρ_{jam} and ρ_{crit} per lane jam density and critical density, respectively. Traffic is in 2 pipe free flow regime when $\rho_1 < \rho_{\text{crit}}$. It is in 2 pipe semi-congestion regime when $\rho_{\text{crit}} \leq \rho_1 < \frac{w_1 \rho_{\text{jam}}}{v_{2,\max} + w_1}$. It is in 1 pipe congestion regime when $\rho_1 \geq \frac{w_1 \rho_{\text{jam}}}{v_{2,\max} + w_1}$. Furthermore, it is assumed that $\rho_2 < \rho_{\text{crit}}$ in the 2 pipe regimes and $\rho_2 < \rho_{\text{jam}}$ in the 1 pipe regime. Therefore, the slow cars will always stay in the outer lane and never enter the inner lane.

4.2.4 Porous Flow Models

The most recent multi-class kinematic wave model are the porous flow models. They consider heterogeneous traffic on a two dimensional roadway. Small vehicles can drive ('creep') through openings ('pores') between other vehicles. It is developed to model disordered traffic flow with different types of vehicles such as cars, scooters and bikes and without lanes. The main idea that if overall densities are low, large vehicles with high maximum velocities (e.g. cars) are faster than smaller vehicles with low maximum velocities (e.g. two-wheelers). However, when the road gets busier, cars are less able to manoeuvre between the other vehicles and two-wheelers are better able to maintain their velocity. The resulting 2-class model by Fan and Work (2015) is very similar to previously developed models with a fundamental diagram that is linear in the density-velocity plane:

$$v_u = \left(1 - \frac{\rho}{\rho_{u,\text{jam}}}\right) v_{u,\max} \tag{4.23}$$

However, class 1 (cars) has a speed in low densities, class 2 (scooters) has a higher velocity in high densities: $v_{1,\max} > v_{2,\max}$ and $\rho_{1,\text{jam}} < \rho_{2,\text{jam}}$, see also Fig. 4.10d. Other examples of porous flow models (Nair et al. 2011; Gashaw et al. 2017) use the same principles but their approach leads to fundamental diagrams with different shapes. However, all porous flow models share the property that at low density one class is faster, while at high density, an other class is faster.

4.2.5 Requirements of Multi-Class Models

Along the same lines of the requirements for fundamental diagrams (Sect. 2.3) and microscopic models (Sect. 3.2.3), requirements for multi-class kinematic wave models are proposed:

1. When the density reaches a certain threshold (which may depend on the traffic composition), all class specific vehicle speeds are zero.
2. When a single vehicle of any class is added to the flow, neither of the class specific speeds will increase.
3. Information travels at finite speed.
4. Information travels at a velocity not larger than that of vehicles.

The first two requirements are similar to the requirements put forward for fundamental diagrams in Sect. 2.3. Especially, the second requirements may seem obvious: when there are more vehicles on the road, they drive slower (or certainly not faster). However, it has been shown that not all multi-class models satisfy this requirements (Van Wageningen-Kessels 2016). Furthermore, the last two requirements relate to hyperbolicity and anisotropy, and 'plausible driver behaviour', like the requirements

in Sect. 3.2.3. A traffic flow model is hyperbolic when it takes time for traffic at some distance to an event, to react to that event: i.e. drivers do not react instantaneously, but after a nonzero reaction time. Along the same lines, drivers only react to their leaders and not to their followers. This is also called anisotropy, as discussed in more detail in Sect. 4.3.1. Some of these requirements are not straightforward to check. However, a step-by-step plan (Van Wageningen-Kessels 2016) can be followed. Application of the plan shows that most models satisfy the requirements, but some only conditionally.

4.3 Higher-Order Models

Higher-order models form the last branch of macroscopic traffic flow models. They include an equation describing the acceleration ('velocity dynamics') towards the equilibrium velocity described by a fundamental relation. In 1971, Payne derived a macroscopic traffic flow model from a simple stimulus-response car-following model. It yields a model consisting of a fundamental relation and two coupled partial differential equations, hence the name higher-order model. The partial differential equations are the conservation of vehicles equation (4.1) and an equation describing the velocity dynamics:

$$\frac{\partial v}{\partial t} + v\frac{\partial v}{\partial x} = \frac{V(\rho) - v}{\tau} - \frac{c^2}{\rho}\frac{\partial \rho}{\partial x} \tag{4.24}$$

with $V(\rho)$ the equilibrium velocity described by the fundamental relation and τ can be interpreted as reaction or relaxation time, because of its relation with the reaction time in the car-following model. c^2 is a diffusion parameter and can for example be chosen to be $c^2 = \mu/\tau$ μ the anticipation coefficient.

4.3.1 Critique on Higher Order Models

Daganzo (1995) has argued that higher-order models are flawed because they are not anisotropic. The main implication of non-anisotropic models is that vehicles may drive backward. To understand this, we note that the term 'anisotropy' in traffic flow theory is used in a slightly different way than usual in fluid dynamics:

Isotropy The fluid flow has no directional preference, e.g. in a water flow, water molecules react the same to their neighbouring molecules independent of in which direction the other molecules are located.

Anisotropy in fluid flows There is a directional preference, e.g. a gravitational force only acts in one direction.

Anisotropy in traffic flows There is a directional preference and vehicles only react on what is happening in front of them, not on what is behind them.

Non-anisotropy in traffic flows There may be a directional preference but vehicles both react to changes in front and behind.

We use the definitions common to traffic flow. In an anisotropic traffic flow, vehicles do not react to what happens behind them. This implies that if a vehicle is in a queue, it does not matter whether there is an other vehicle behind them or not, it will just stay in the queue and only start moving once the vehicles in front start moving. In a non-anisotropic traffic flow, however, this same vehicle in a queue may behave differently depending on what happens behind them. If there is no vehicle behind them, in a non-anisotropic model, the vehicle may start to drive backward. This is usually due to the diffusion term $-\frac{c^2}{\rho}\frac{\partial \rho}{\partial x}$. An other property of non-anisotropic traffic flow models is related to the characteristic velocity at low densities and high vehicle speeds. In a non-anisotropic model, again the diffusion term $-\frac{c^2}{\rho}\frac{\partial \rho}{\partial x}$ causes behaviour that is considered unrealistic, namely characteristics travelling faster than the average vehicle speed. This is explored further in Problems 4.6 and 4.8.

The introduction of the concept of anisotropy in traffic flow by Daganzo (1995) sparked a long debate on whether or not traffic flow models should be anisotropic, in which Helbing (2009) gave the final contribution. Some authors (e.g. Zhang (2003)) argue that in multi-lane traffic, the average vehicle speed can be below the speed of the fastest vehicles and therefore, those fastest vehicles can carry information with them at a speed higher than the average vehicle speed. This would make characteristics travelling faster than the average speed realistic on multi-lane roads, as long as the characteristics are not faster than the fastest vehicles.

4.3.2 Anisotropic Higher Order Models

In the time Daganzo's article was written, existing higher-order models were indeed not anisotropic. The publication has lead to rapid developments of new higher order models that resolve the problems by including an other speed equation. Probably the most well-known of them is the ARZ model by Aw and Rascle (2000); Zhang (2002) with:

$$\frac{\partial v}{\partial t} + v\frac{\partial v}{\partial x} = -c(\rho)\frac{\partial v}{\partial x} \tag{4.25}$$

with $c(\rho) = \rho V'(\rho)$ the 'sound speed': the speed at which a small perturbation travels. In this and similar models, when parameters have been chosen reasonably, characteristic waves can not be faster than vehicles. This is explored further in Problems 4.6, 4.7 and 4.8. Extended versions of this model have been proposed to include multiple classes or multiple lanes.

4.3.3 Generic Higher Order Model

Lebacque et al. (2007) develop a generalized higher-order model (GSOM) that includes the models such as those by Aw and Rascle (2000); Zhang (2002) as special cases. It includes a 'generic invariant' I, which is attached to the vehicle stream and could thus be seen as a property of a vehicle or driver: every vehicle may have a different function $\tilde{I}(t, x)$. The main idea is that $\tilde{I}$ may depend on the actual traffic state $\tilde{I}(t, x) = I(\rho(t, x), v(t, x))$, but this function I travels with the vehicles. For example, I could model slow acceleration for some vehicles and fast acceleration for others, and thus changing the fundamental diagram.

The generalized model is as follows:

$$\frac{\partial \rho}{\partial t} + \frac{\partial q}{\partial x} = 0 \tag{4.26a}$$

$$\frac{\partial}{\partial t}(\rho I) + \frac{\partial}{\partial x}(q I) = -\rho g(I) \tag{4.26b}$$

$$I = I(\rho, v) \tag{4.26c}$$

Note that only if $f(I) = 0$, the invariant is actually conserved over vehicle trajectories. If the relaxation function $f(I)$ is nonzero, than I is not conserved but, depending on the choice of the relaxation function, it changes slowly. A slight adaptation of the ARZ model is presented as a typical example within the GSOM with the invariant the distance to the equilibrium fundamental relation:

$$I = v - V(\rho) \tag{4.27}$$

and the relaxation term models acceleration/deceleration towards the equilibrium fundamental relation:

$$g(I) = \frac{I}{\tau} \tag{4.28}$$

For later reference, we note that the generic model (4.26) can be reformulated as a system of conservation equations:

$$\frac{\partial \mathbf{u}}{\partial t} + \mathrm{J}(\mathbf{u}) \frac{\partial \mathbf{u}}{\partial \mathrm{x}} = s(\mathbf{u}) \tag{4.29}$$

with state vector, Jacobian and source function, respectively:

$$\mathbf{u} = \begin{pmatrix} \rho \\ I \end{pmatrix}, \quad \mathrm{J}(\mathbf{u}) = \begin{pmatrix} \frac{\mathrm{d}q}{\mathrm{d}\rho} & 0 \\ 0 & v \end{pmatrix} = \begin{pmatrix} v + \rho \frac{\mathrm{d}v}{\mathrm{d}\rho} & 0 \\ 0 & v \end{pmatrix} \quad \text{and} \quad \mathrm{s}(\mathbf{u}) = \begin{pmatrix} 0 \\ -g(I) \end{pmatrix} \tag{4.30}$$

To see the equivalence between (4.26) and (4.29), we rewrite (4.26b):

$$\rho \frac{\partial I}{\partial t} + I \frac{\partial \rho}{\partial t} + q \frac{\partial I}{\partial x} + I \frac{\partial q}{\partial x} = -\rho g(I) \tag{4.31}$$

Substitution (4.26) and dividing by ρ gives:

$$\frac{\partial I}{\partial t} + v \frac{\partial I}{\partial x} = -g(I) \tag{4.32}$$

Combining (4.26) and (4.32) yields (4.29).

Furthermore, in certain cases, it is useful to rewrite the second term of (4.29) as a partial derivative of the flux function $f(\mathbf{u})$:

$$\frac{\partial f(\mathbf{u})}{\partial x} = \mathrm{J}(\mathbf{u}) \frac{\partial \mathbf{u}}{\partial \mathrm{x}} = \begin{pmatrix} \frac{\mathrm{d}q}{\mathrm{d}\rho} & 0 \\ 0 & v \end{pmatrix} \frac{\partial \mathbf{u}}{\partial \mathrm{x}} = \begin{pmatrix} \frac{\mathrm{d}q}{\mathrm{d}\rho} \frac{\partial \rho}{\partial x} \\ v \frac{\partial I}{\partial x} \end{pmatrix} \tag{4.33}$$

This then yields the conservative form of (4.26):

$$\frac{\partial \mathbf{u}}{\partial t} + \frac{\partial f(\mathbf{u})}{\partial x} = s(\mathbf{u}) \tag{4.34}$$

4.4 Moving Coordinates

Traditionally, macroscopic traffic flow models are formulated in the Eulerian—fixed—coordinate system. This is also the approach that has been taken in this chapter until now. In the fixed coordinate system, the independent variables are time t and position x, see Fig. 4.12a. Traffic state variables, such as density, flow and speed, are expressed as function of time and location. Discretizations are used in simulations (more details in Chap. 5) and involve calculating the state variables on fixed times and at fixed locations. However, this is not the only possible approach and other approaches have some advantages.

4.4.1 The Lagrangian Coordinate System

Since the early 2000s several authors have developed macroscopic models formulated in the Lagrangian—moving—coordinate system (Aw et al. 2002; Leclercq et al. 2007; van Wageningen-Kessels et al. 2010). In the moving coordinate system, the independent variables are time t and vehicle number n, see Fig. 4.12b. Traffic state variables are expressed as function of time and vehicle number. This results in the following conservation equation:

$$\frac{\mathrm{D}s}{\mathrm{D}t} + \frac{\partial v}{\partial n} = 0 \tag{4.35}$$

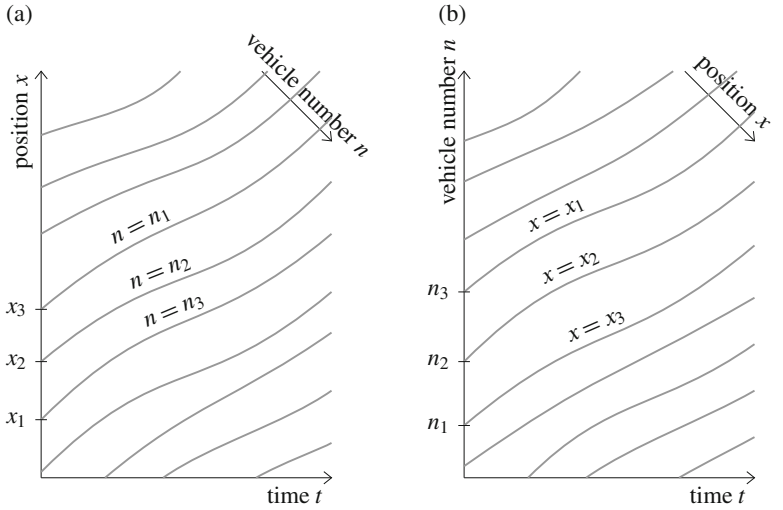

Fig. 4.12 Trajectories in Eulerian and Lagrangian coordinate system. (**a**) Eulerian coordinate system with vehicle trajectories: vehicle number n increases over time t for a fixed position x. (**b**) Lagrangian coordinate system with vehicle trajectories: position x increases over time t for a fixed vehicle number n

Table 4.2 Comparison of different formulations of the kinematic wave model

	Euler	Lagrange
Coordinates	(x, t)	(n, t)
Main state variable	$\rho = -\partial n/\partial x$	$s = -\partial x/\partial n$
Fundamental relation	$q = Q(\rho)$	$v = V(s)$
Conservation equation	$\frac{\partial \rho}{\partial t} + \frac{\partial q}{\partial x} = 0$	$\frac{\mathrm{D}s}{\mathrm{D}t} + \frac{\partial v}{\partial n} = 0$

The conservation equation in Lagrangian formulation (4.35) can be understood qualitatively by considering two vehicles: a leader and a follower. If the follower has a higher velocity than the leader, the distance between the two vehicles decreases, i.e. if $\partial v/\partial n > 0$ then $\mathrm{D}s/\mathrm{D}t < 0$. The reverse is also true: if the follower is slower than the leader the distance will increase.

For easy reference, the Eulerian and Lagrangian formulation of the kinematic wave model are summarized in Table 4.2. The advantages of this moving coordinate system include simpler extensions of the model in certain directions (e.g. including bounded acceleration, see Sect. 4.5) faster and more accurate calculations (see Sect. 5.4) and easier analysis of the models (Van Wageningen-Kessels 2016). However, there is a third formulation of the kinematic wave model—the 'T-model'—that uses space and vehicle number as independent variables (Laval and Leclercq 2013).

4.4.2 Graphical Derivation

The Lagrangian conservation equation can be derived using a similar procedure as the derivation of the kinematic wave model in Eulerian coordinates (Sect. 4.1.1). Alternatively, the model can be derived analytically from the Eulerian formulation. We focus on the graphical approach, which may be more intuitive and easy to understand. In Problem 4.14, we encourage the interested reader to also study the analytical approach, which is mathematically more rigorous.

In the Lagrangian case, the control volume is not rectangular as in Fig. 4.1 but it is a platoon of Δn vehicles that is followed over a time Δt, as in Fig. 4.13. However, the platoon is rectangular in the (t, n)-plane. The road length taken by this platoon changes over time as it travels forward. On one hand, the original length at time t_1 is increased by the distance traveled by the first vehicle n_1. On the other hand, it is decreased by the distance traveled by the last vehicle $n_2 = n_1 + \Delta n$. (Note again the order of vehicles: vehicle n_2 is behind vehicle n_1.) This can be written as:

$$\underbrace{\int_{n_1}^{n_2} s(t_2, n)\mathrm{d}n}_{\text{final length}} = \underbrace{\int_{n_1}^{n_2} s(t_1, n)\mathrm{d}n}_{\text{initial length}} + \underbrace{\int_{t_1}^{t_2} v(t, n_1)\mathrm{d}t}_{\text{distance first veh}} - \underbrace{\int_{t_1}^{t_2} v(t, n_2)\mathrm{d}t}_{\text{distance last veh}}. \quad (4.36)$$

Again, by decreasing the control volume to an infinitesimal volume we may assume spacing s and velocity v are constant within this volume. Consequently,

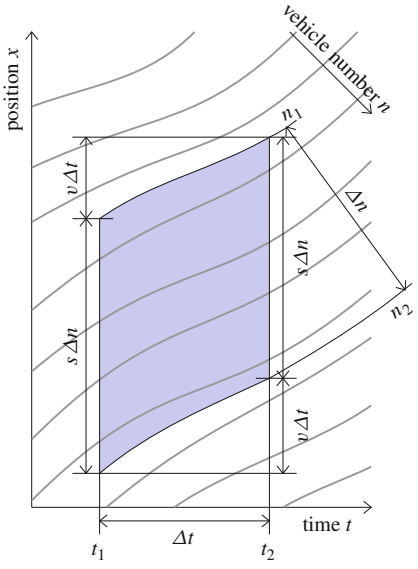

Fig. 4.13 Graphical derivation of the conservation equation in the kinematic wave model in Lagrangian coordinates, using vehicle trajectories and a control volume

$\int_{n_1}^{n_2} s(t,n)\mathrm{d}n \to s(t,n)\Delta n$ and $\int_{t_1}^{t_2} v(t,n)\mathrm{d}t \to v(t,n)\Delta t$. Furthermore, rewriting (4.36) yields:

$$\frac{s(t_2,n_1)-s(t_1,n_1)}{\Delta t}+\frac{v(t_2,n_2)-v(t_2,n_1)}{\Delta n}=0. \tag{4.37}$$

We take an infinitesimal volume, that is: we let $\Delta n \to 0$ and $\Delta t \to 0$ in (4.37). Furthermore, we use the definition of the partial derivative (4.4) to find the Lagrangian conservation equation (4.35).

4.4.3 Generic Higher Order Model in Lagrangian Coordinates

The generic higher order model (4.26) lends itself well for reformulation in the Lagrangian coordinate system. This is because the driver attribute I travels with the vehicles and thus the model becomes:

$$\frac{\mathrm{D}s}{\mathrm{D}t}+\frac{\partial v}{\partial n}=0, \tag{4.38a}$$

$$\frac{\mathrm{D}I}{\mathrm{D}t}=-g(I), \tag{4.38b}$$

$$v=V(s,I) \tag{4.38c}$$

4.5 Bounded Acceleration, Hysteresis and Capacity Drop

One of the most common critiques on the LWR model is the underlying assumption of instantaneous acceleration and deceleration. This implies, for example, that when a vehicle leaves congestion and enters a free flow region, according to the LWR model it would accelerate instantaneously to its free flow speed. This problem is fixed in higher order models, however, also more direct ways to address it have been introduced. These adaptations to the LWR model include bounded accelerations. Usually, only acceleration is bounded because instantaneous deceleration proves to be less of in issue in practise. However, the same techniques could be applied the also limit deceleration.

4.5.1 Bounded Acceleration

It is most natural to introduce bounded acceleration in the Lagrangian coordinate system. This is because the coordinates move with the vehicles and one can just

limit their change in speed. This idea was introduced by Leclercq (2009) and further developed by others including Calvert et al. (2015), Calvert et al. (2018). The simplest version of a bounded acceleration model limits the acceleration by explicitly requiring the speed to be as large as possible under the constraints of the fundamental diagram and the bounded acceleration. I.e. speed v is maximised such that both:

$$v \leq V(1/s) \quad \text{and} \quad \frac{\partial v}{\partial t} \leq a_{\max} \tag{4.39}$$

with $a_{\max} > 0$ the maximum acceleration.

The main advantage of doing this in the Lagrangian coordinate system lies in the discretisation. This is because, very much like in a car-following model, trajectories are calculated and the bounded acceleration condition makes them more smooth, as in Fig. 4.14. The discretisation will be discussed in more detail in Chap. 5.

Alternatively, bounded acceleration can be introduced in the Eulerian coordinate system, even though that is a bit more complicated. In such cases, the numerical

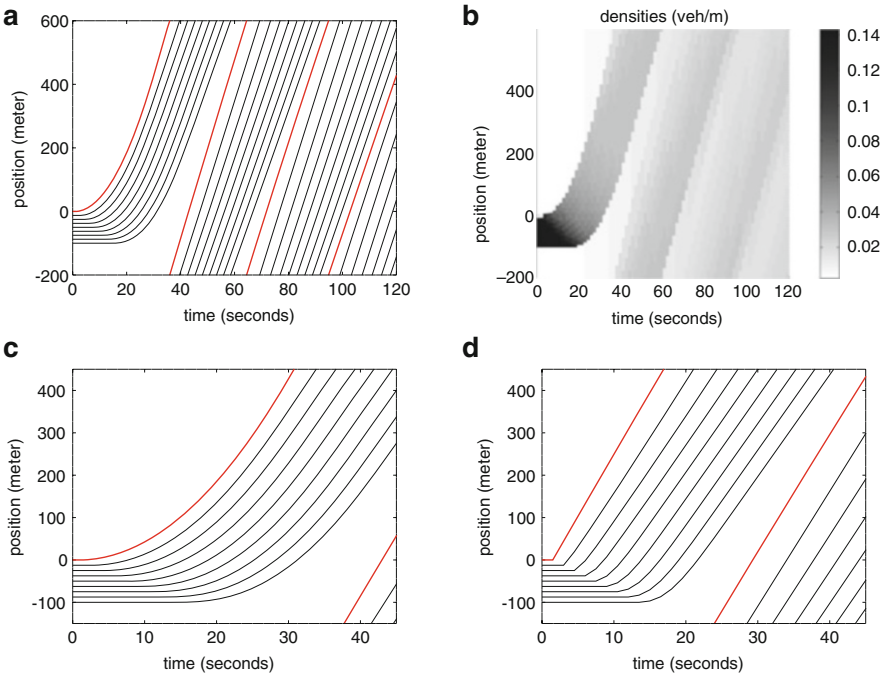

Fig. 4.14 Simulation results with bounded acceleration and comparison of trajectories (zoomed) with and without bounded acceleration. (**a**) Trajectories. (**b**) Densities. (**c**) Trajectories with bounded acceleration (zoom of (**a**). (**d**) Trajectories without bounded acceleration (zoom of Fig. 4.9a)

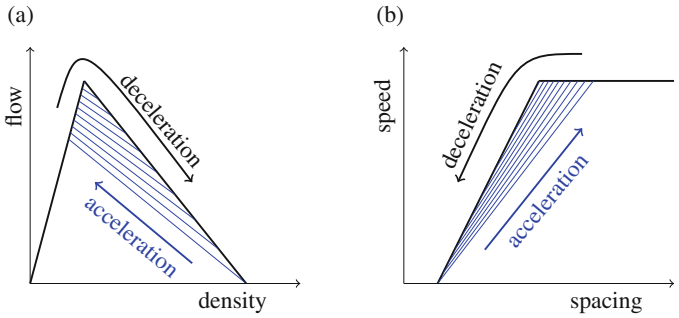

Fig. 4.15 Fundamental relation with hysteresis: the black line is the original fundamental diagram, that is active during deceleration. When traffic accelerates, however, one of the other branches—with reduced flow and speed—is followed. (**a**) Density-flow: for model in Eulerian formulation. (**b**) Speed-spacing: for model in Lagrangian formulation

solution method is altered to account for the capacity drop (Lebacque 2003; Srivastava and Geroliminis 2013).

4.5.2 Hysteresis

An other way to model the hysteresis effect, is to include multiple branches in the fundamental diagram: one congestion branch for deceleration and one (or even more) for acceleration. Instead of using the speed in the original fundamental diagram, in the acceleration phase, the speed is reduced to a lower branch, as indicated in Fig. 4.15. It is recommended that the Lagrangian coordinate system is applied for simulation (Yuan et al. 2017).

Problem Set

Method of Characteristics

Consider the following initial value problem. Initially, traffic state is as follows:

$$\rho(x,0) = \begin{cases} 0 & \text{if } x > 0 \\ \rho_{\text{jam}} & \text{if } -200 \leq x \leq 0 \\ 0 & \text{if } x < 200 \end{cases} \tag{4.40}$$

Furthermore, the LWR model is applied, in combination with a bilinear fundamental diagram, with parameters as in Table 4.1, except for critical speed $v_{\text{crit}} = v_{\text{max}} = 30$ m/s.

4.1 Apply the method of characteristics to solve the initial value problem. Draw the traffic states in the (t, x)-plane and answer the following questions:

1. At any $t > 0$, what is the velocity of the first vehicle that starts driving?
2. What is the velocity of the downstream front of the queue?
3. What is the velocity of the upstream front of the queue?
4. How long does it take for the queue to solve?

Consider the same problem as above, but now with – in addition to the prescribed initial densities as in (4.40) – the following upstream boundary conditions:

$$q(400, t) = \begin{cases} 0 & \text{if } 0 < t < 6.67 \\ \rho_{\text{crit}} v_{\text{max}} & \text{if } 6.67 \leq t \leq 20 \\ 0 & \text{if } t > 20 \end{cases} \quad \text{and}$$

$$\rho(400, t) = \begin{cases} 0 & \text{if } 0 < t < 6.67 \\ \rho_{\text{crit}} & \text{if } 6.67 \leq t \leq 20 \\ 0 & \text{if } t > 20 \end{cases} \tag{4.41}$$

This can be interpreted as a platoon of vehicles that approaches the queue, for example from a traffic light further upstream.

4.2 Apply the method of characteristics to solve the combined initial and boundary value problem. Draw the traffic states in the (t, x)-plane.

Simulations

Simulations can give better insights into models. Sample code can be found on the website (http://extras.springer.com) of this book.

4.3 Run a simulation to reproduce the results in Fig. 4.9.

4.4 Adapt the code to apply the bilinear fundamental diagram instead of the parabolic linear one. Reflect on the results and comment on whether they are in correspondence with the solution of problem 4.1.

4.5 Adapt the provided code in one or more of these directions:

- make the initial queue longer
- change parameter values of the model parameters (maximum speed, critical speed, jam density, critical density)
- change to yet an other fundamental diagram

Compare the results of different setups and write about your insights: is this more (or less) realistic? Do you see other phenomena? Compare your results with those in literature.

The reader is further encouraged to run different simulations in the problem set of the next chapter, after introducing the numerical methods.

Higher Order Models

As discussed in Sect. 4.3, the Payne model ((4.1) and (4.24)) is not anisotropic, while the ARZ ((4.1) and (4.25)) is. To calculate the characteristic velocities, the models are reformulated into a system of equations (4.42):

$$\frac{\partial \mathbf{u}}{\partial t} + \mathrm{J}(\mathbf{u})\frac{\partial \mathbf{u}}{\partial \mathrm{x}} = \mathrm{f}(\mathbf{u}) \tag{4.42}$$

with the state vector $\mathbf{u} = \begin{pmatrix} \rho \\ y \end{pmatrix}$, $J(\mathbf{u})$ the jacobian matrix and $f(\mathbf{u})$ the source term. The variable y and the Jacobian matrix are different for each model. The eigenvalues of the Jacobian matrix are the characteristic values.

4.6 Calculate the characteristic velocities of the Payne model by:

1. Define variable y, the Jacobian matrix $\mathrm{J}(\mathbf{u})$ and the source term $f(\mathbf{u})$ such that (4.42) defines the Payne model.
2. Determine the eigenvalues of the Jacobian matrix.

4.7 Calculate the characteristic velocities of the ARZ model.

4.8 Reflect on the difference between the Payne model and the ARZ model and on why the first one is not anisotropic and the second one is.

An other popular model is the Aw-Rascle model (Aw and Rascle 2000) with the following speed equation:

$$\frac{\partial}{\partial t}(v + p(\rho)) + v\frac{\partial}{\partial x}(v + p(\rho)) = 0 \tag{4.43}$$

with $p(\rho)$ a 'pressure term'. The (increasing) function $p(\rho)$ can have different forms, but $p(\rho) = \rho^c$ with some constant $c > 0$ is considered as the prototype.

4.9 (Advanced) Calculate the characteristic velocities of the Aw-Rascle model.

4.10 (Advanced) Define the invariant I and the source function $g(I)$ for the Aw-Rascle model, i.e.: for which functions $I(\rho, v)$ and $g(I)$ in the generic higher order model, is the Aw-Rascle model retrieved?

Models with Capacity Drop/Hysteresis

4.11 (Advanced) Run a simulation to reproduce the results in Fig. 4.14.

4.12 (Advanced) Adapt the code to use the bilinear fundamental diagram and reflect on how the results differ from the ones with the linear-parabolic fundamental diagram, and from the ones without bounded acceleration.

4.13 (Advanced) Adapt the code to apply other maximum accelerations and reflect on how the simulation results change.

The Lagrangian Coordinate System

The Lagrangian formulation of the LWR model (4.35) can be derived from its Eulerian formulation (4.1). Therefore, the definition of spacing and the Lagrangian time derivative are needed. The definition of spacing expresses spacing as the partial derivative of the position x to vehicle number n:

$$s = \frac{1}{\rho} = -\frac{\partial x}{\partial n} \tag{4.44}$$

The minus sign results from the fact that vehicles are numbered opposite to the driving direction. Furthermore, the Lagrangian time derivative is:

$$\frac{\mathrm{D}}{\mathrm{D}t} = \frac{\partial}{\partial t} + v\frac{\partial}{\partial x} \tag{4.45}$$

$\mathrm{D}/\mathrm{D}t$ is the partial derivative with respect to time in Lagrangian coordinates, that is: the derivative with respect to time t with the other coordinate (vehicle number n) fixed. As n-coordinates move with vehicle velocity, $\mathrm{D}r/\mathrm{D}t$ is the rate of change of some variable r as it is observed by a driver moving with velocity $v(n,t) = v(x(n),t) = \partial x/\partial t$. This implies that $\mathrm{D}/\mathrm{D}t$ is a directional derivative in Eulerian coordinates: it is the derivative in the direction of the moving observer (the driver). Both coordinates t and x change in this direction. Conversely, $\partial/\partial t$ is a partial derivative in Eulerian coordinates and a directional derivative in Lagrangian coordinates.

4.14 (Advanced) Derive the Lagrangian formulation of the LWR model from its Eulerian formulation. Hint: Use (4.44) to redefine density as a partial derivative and substitute it into the Eulerian conservation equation. After reordering the result, substitute the Lagrangian time derivative (4.45) and apply the definition of spacing once again.

The Lagrangian formulation can also be applied to higher order models and multi-class kinematic wave models (van Wageningen-Kessels et al. 2010).

4.15 (Advanced) Derive the Lagrangian formulation (4.38) of the generic higher order model (4.26) or of a multi-class model.

Further Reading

Aw A, Klar A, Rascle M, Materne T (2002) Derivation of continuum traffic flow models from microscopic follow-the-leader models. SIAM J Appl Math 63(1):259–278

Lebacque JP, Mammar S, Haj Salem H (2007) Generic second order traffic flow modelling. In: Allsop RE, Bell MGH, Heydecker BG (eds) Transportation and traffic theory 2007. Elsevier, Oxford, pp 755–776

Leclercq L, Laval J, Chevallier E (2007) The Lagrangian coordinates and what it means for first order traffic flow models. In: Allsop RE, Bell MGH, Heydecker BG (eds) Transportation and traffic theory 2007. Elsevier, Oxford, pp 735–753

Van Wageningen-Kessels FLM (2016) Framework to assess multi-class continuum traffic flow models. Transp Res Rec J Transp Res Board 2553:150–160